Received: 2 July 2020 | Revised: 3 September 2020 | Accepted: 13 September 2020

DOI: 10.1002/we.2572

RESEARCH ARTICLE

WILEY

Analysis of the influence of climate change on the fatigue lifetime of offshore wind turbines using imprecise probabilities

Clemens Hübler | Raimund Rolfes

Institute of Structural Analysis, Leibniz Universität Hannover, Hannover, Germany

Correspondence
Clemens Hübler, Leibniz Universität Hannover, Institute of Structural Analysis, ForWind, Appelstr. 9a, Hannover D-30167, Germany.
Email: c.huebler@isd.uni-hannover.de

Funding information
Deutsche Forschungsgemeinschaft, Grant/Award Number: 436547100

Abstract

When discussing the connection of wind energy and climate change, normally, the potential of wind energy to reduce green house gas emissions is emphasised. Hence, effects of wind energy on climate change are analysed. However, what about the other direction? What is the impact of climate change on wind energy? Recently, the effect of a reversal in global terrestrial stilling,that is, an increase in global wind speeds in the last decade, on the wind energy production has been analysed. Certainly, knowledge about potential changes in energy production is essential to plan future energy supply. Nonetheless, at least similarly important is the effect on loads acting on wind turbines. Increasing loads due to higher wind speeds might reduce wind turbine lifetimes and yield higher costs. Moreover, especially for already existing turbines, it might even affect the structural reliability. Since the impact of climate change on wind turbine loads is largely unknown, it is studied in this work in more detail. For this purpose, different existing models for predicted changes in wind speed and air temperature and their uncertainties are used to forecast the environmental conditions an exemplary offshore wind turbine is exposed to. Subsequently, for this turbine, the lifetime fatigue damages are calculated for different prediction models. It is shown that the expected changes in lifetime fatigue damages are present but relatively small compared to other uncertainties in the fatigue damage calculation.

KEYWORDS

climate change, fatigue, imprecise probabilities, scattering environmental conditions, uncertainty, wind energy

1 | INTRODUCTION

Wind energy in general and offshore wind energy in particular are supposed to be major clean energy sources in future[1] to reduce green house gas emissions, and therefore, to stop or at least limit climate change. However, even today, we already witness a significant amount of climate change.[2,3] For the upcoming years, further changes are predicted.[4,5] Therefore, there is also a significant amount of research focussing on effects of climate change on wind energy. A comprehensive summary of these effects is given by Pryor and Barthelmie.[6] Such research aims, inter alia, at answering the question whether these changes will help us to achieve the objectives set with respect to wind energy production or will rather aggravate the situation.

[Correction added on 07 November 2020, after first online publication: Projekt Deal funding statement has been added.]

In this context, global terrestrial stilling has been a major concern in the past years. Stilling describes the phenomenon of reducing average wind speeds over land.[7] It was observed worldwide from the 1980s to around 2010.[8,9] Decreasing wind speeds lead to a reduced energy production.[9,10] Hence, even more wind turbines would be needed. However, for some local areas, especially offshore, this global trend was irrelevant. One of these areas, which is of particular relevance for the offshore wind energy sector, is the North Sea. For the North Sea, the effect of climate change on wind and waves has been studied comprehensively.[11,12] Increasing wind speeds were already predicted 10 years ago for the Neath Sea.[13] Moreover, it has been found out recently that global terrestrial stilling reversed around 2010.[14] Hence, even onshore, increasing wind speeds are now predicted for the upcoming years. This increases the wind energy potential significantly. Zeng et al[14] calculated an increased hypothetical global production potential of more than 15% for the years 2010 to 2017.

On the one hand, this predicted increase in wind speeds might help us to achieve the objectives set with respect to wind energy production by increasing the wind potential. This effect has already been investigated in many studies.[14,15] On the other hand, higher wind speeds do not only yield higher energy outputs but also increase wind loads acting on the turbines. That is why, future wind turbines will probably have to be designed for higher loads, and therefore, the cost of wind energy might increase. Moreover, perhaps even more relevant, current wind turbines are not designed for these higher wind speeds. Although wind turbines are designed with significant safety factors,[16] the expected harsher wind conditions might reduce the reliability of current turbines. This means that lifetimes might be reduced. In some rare cases, the structural integrity can even be endangered. These effects of climate change on wind turbine loads, especially of the recently predicted higher wind speeds, have not yet been analysed in detail. The impact of climate change on wind turbine loads is largely unknown. Some early work on this topic was conducted by Clausen et al[17,18] However, Clausen et al. did not focus on fatigue loads. For their fatigue analysis, they used a highly simplified approach by neglecting wave loads and considering only two load cases. Recently, Bisoi and Haldar[19,20] analysed the effect of climate change on the dynamic behaviour of offshore wind turbines. They investigated the effect of increasing maximum wind speeds on ultimate and fatigue loads based on a simplified beam model of a wind turbine. Their fatigue analysis is based on the annual maximum wind speed only and not on the entire wind speed distribution or even on the joint distribution of various environmental conditions. Hence, so far, all research on the effect of climate change on fatigue lifetimes of wind turbines is based on highly simplified structural models and/or load cases. As a consequence, it is studied in more detail and in consideration of uncertainties in this work to answer the following question: What is the influence of climate change on wind turbine fatigue loads and is it relevant for the lifetime calculation?

For this purpose, for an exemplary offshore wind turbine located in the North Sea, the environmental conditions the turbine is exposed to over its entire lifetime are forecasted using various models for climate change. For these models, their inherent uncertainty is taken into account. Subsequently, for this turbine, fatigue loads are calculated for the different prediction models. This enables an investigation of the impact of climate change on the fatigue lifetime of offshore wind turbines. Finally, the results and their uncertainty are compared to the uncertainty in lifetime predictions in general. This helps to estimate the relevance of climate change for wind turbine fatigue lifetime calculations.

The rest of this work is structured as follows: In Section 2, first, the exemplary wind turbine site including the present environmental conditions is described. Second, several existing models for predicted changes in wind speed and air temperature are presented. And third, it is shown how their uncertainties can be modelled using imprecise probabilities. Section 3 focusses on the fatigue lifetime calculation. First, a measure for the fatigue lifetime is introduced and explained. It is the lifetime damage equivalent load (DEL). Second, the applied model for the exemplary wind turbine is presented. Since the computation of lifetime DELs is quite time-consuming, third, a meta-model-based approach is introduced. This approach enables a fairly efficient calculation of lifetime DELs. In Section 4, the outcomes of the analyses of the environmental conditions including predicted changes and uncertainties are presented. Moreover, resulting DELs and their uncertainties are discussed and compared to uncertainties related to the DEL computation. Finally, in Sections 5 and 6, the benefits and limitations of this work are discussed and conclusions are drawn.

2 | MODELS FOR ENVIRONMENTAL CONDITIONS

Predicted climate changes vary significantly with respect to their characteristic and extent between different areas. Even in Europe or the North Sea, predictions are not uniform. For example, for some parts of Europe and the North Sea, increasing wind speeds and for others declining ones are predicted.[10,13] Therefore, it is not possible to investigate the impact of climate change on the fatigue lifetime of wind turbines in general. That is why an exemplary offshore site and a corresponding generic wind turbine are chosen for this analysis. As a result, complete universal validity cannot be claimed for the conclusions of this study. Nonetheless, due to the consideration of uncertainties and the selection of a site that is representative for many offshore wind turbines in Europe, trends are generally valid.

2.1 | Exemplary offshore site

The selected exemplary offshore site is the location of the FINO3 measurement platform in the North Sea (see Figure 1). This selection has several advantages. First, the location is close to various offshore wind farms. Hence, it is representative for many real offshore wind turbines.

FIGURE 1 Position of the FINO3 platform in the North Sea, adapted from OpenStreetMap [Colour figure can be viewed at wileyonlinelibrary.com]

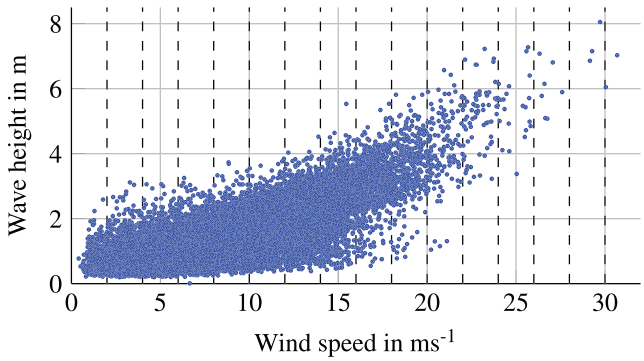

FIGURE 2 Scatter plot of the measured wind speeds and wave heights at FINO3 within the 8-year period to illustrate dependencies [Colour figure can be viewed at wileyonlinelibrary.com]

Second, the measurement mast delivers a large amount of high-quality measurements of environmental conditions. And third, several regional predictions for the expected climate changes have already been made for the North Sea.

At FINO3, inter alia, maximum, minimum, mean and standard deviation values of the wind speed, measured at different heights between 30 and 100 m above mean sea level, are available for 10-min intervals (see Appendix A for information regarding the data availability). Wind speeds are measured with cup and ultrasonic anemometers. In this study, cup anemometers are used. Three anemometers are installed around the mast to minimise shadow effects. In addition, 10-min mean values for humidity, air pressure and air temperature are accessible. Thus, air densities can be calculated. A buoy in the immediate vicinity of the research platform (about 150 m) measures wave conditions. For example, mean values of significant wave heights and wave peak periods are recorded every 30 min. The FINO3 platform has been measuring continuously since 2009. Here, a measurement period of 8 years (1 December 2010 to 30 November 2018) is considered. More detailed information regarding the measurements at FINO3 can be found, for example, on the website.[21] The postprocessing of the raw data, for example, the reduction of tower shadow effects or the computation of air densities is explained in Hübler et al.[22]

Before adding climate change effects for the upcoming years, the present situation has to be described, Hence, for the FINO3 site, theoretical statistical distributions for several important environmental conditions (wind speed (v), wave height (H_s), wave period (T_p) and air density (ρ)) are derived using the postprocessed data. The selection of these four environmental conditions is based on previous studies[23] or is due to the pronounced predicted changes (cf. Section 2.2). Other environmental conditions, like wind-wave-misalignment or turbulence intensities, are either modelled as constant or fully correlated without an own scatter (e.g., the turbulence intensity is modelled as a function of the wind speed). Since environmental conditions are not independent of each other, correlations between them have to be considered. In this work, wind speed and air density are regarded as independent inputs. Wave heights depend on wind speeds. Wave periods depend on the wave height. Exemplarily, the dependency of wind speed and wave height is shown in Figure 2.

To cover the described dependencies of the environmental conditions, joint statistical distributions are commonly used.[24–27] For this purpose, in most cases, the data are divided into bins. This means: For the wind speed and air density, the entire data are utilised to fit theoretical statistical distributions. However, for the wave height, the data are divided into bins of 2 ms^{-1} wind speed (marked in Figure 2). For each bin, an individual distribution is fitted. This yields a noncontinuous joint distribution (cf. Figure 6 (right)). Applying an additional step, interpolations (e.g., regressions) across the various bins can be used to create continuous joint distributions.[26,27] In this work, we abstain from this additional step and use noncontinuous joint distributions, which is a standard approach for wind turbine modelling.[24,25] Similar to the wave height, for the wave period, the data are split up into bins of 0.5 m wave height. In each bin or for the entire data, if no binning is applied, several theoretical statistical distributions are fitted to the data. For example, normal distributions, Gumbel distributions, etc. are fitted. Distribution parameters (e.g., μ and σ for the normal distribution) are determined using a maximum likelihood estimation. Since several distributions are fitted, $\mathcal{X}^2$ tests are conducted in a second step to determine which theoretical statistical distribution fits the data best. This approach of fitting dependent statistical distributions has already been successfully applied in Hübler et al[22] for a similar data set. There, additional explanations can be found.

2.2 | Models for climate change

For classical wind turbine designs, statistical distributions of environmental conditions are used as a basis for lifetime calculations. The distributions are derived using measurement data of past years, as described in the previous section. However, this approach is actually only valid, if insignificant long-term changes are assumed. In the introduction, it is outlined that current research clearly indicates that climate change will influence these distributions in the long term. Therefore, models to predict these changes are required. The intention of this work is not to develop any new prediction models. Instead, it applies three different existing predictions. Since wind conditions are design-driving for wind turbines, the first two models are related to wind speed predictions. One model focusses on local predictions for the North Sea, while the other one analyses the most recent global trends. The third one describes global warming, that is, air temperature predictions. The air temperature has an indirect impact on wind turbine loads. Increasing air temperatures (T) lead to decreasing air densities (ρ) according to the following equation:

$$\rho = \frac{p}{R_{\text{specific}} T}, \tag{1}$$

where p is the air pressure and R_{specific} is the specific gas constant. Moreover, the rotor thrust (F_T) is not only proportional to the square of the wind speed (v) but also to the air density:

$$F_T \sim \rho v^2. \tag{2}$$

Hence, it can be expedient to analyse not only the effect of long-term changes in wind speeds but also of air temperatures.

2.2.1 | Extreme wind conditions in the North Sea

The first prediction model is based on the work of Grabemann and Weisse.[13] Grabemann and Weisse[13] predict wind and wave conditions for the North Sea for the end of the century (2071–2100). Not only the change of the median is predicted but also changes of the 99th percentile. While changes of extreme events can be neglected in energy production predictions, they might be relevant for load calculations. The predictions are based on simulation results of two different general circulation models (GCMs) in combination with two different emission scenarios. See Grabemann and Weisse[13] for more details.

For the FINO3 location, an increase of 0.45 to 1.025 ms^{-1} of the 99th percentile of the wind speed distribution is predicted within the next approximately 90 years. The range of values is a result of the model uncertainty due to different GCMs and emission scenarios. The median wind speed is forecasted to change insignificantly by about 0.075 ms^{-1}. Due to the model uncertainty, even a small decrease of the median is possible. Since no information regarding the type of distribution is given, we assume that it does not change. Grabemann and Weisse[13] give predictions for wave conditions as well. These predictions are not used for the present work, since wave conditions are modelled as dependent variables. Hence, increasing wind speeds already result in higher wave heights. This increase is in the same order of magnitude as predicted by Grabemann and Weisse.[13]

2.2.2 | Reversed global terrestrial stilling

The second prediction model is proposed by Zeng et al.[14] They discovered increasing wind speeds all over the world during the last few years. Based on a purely data-driven approach, an increase of the mean wind speed of 0.24 ms^{-1} per decade is predicted. The uncertainty of this prediction is given as $\sigma = 0.03\ ms^{-1}$. Hence, based on a 4σ interval, the expected increase is between 0.12 and 0.36 ms^{-1} per decade. Regarding extreme

values, no information is given. In this work, we therefore assume that the 99th percentile increases accordingly and the type of distribution remains the same. This simplification requires approval in future research.

2.2.3 | Air temperature in the North Sea

The last prediction model focusses on air temperature changes due to global warming. It is based on the work of Giorgi et al.[5] Similar to Grabemann and Weisse,[13] predictions for the period 2071–2100 were made. Moreover, the same two emission scenarios were analysed. The predictions are based on simulations of a regional climate model (RCM) nested within a GCM. Predictions are given for summer and winter months separately. For details, it is referred to Giorgi et al.[5] For the FINO3 location, an increase of 1.8 to 2.9 K of the air temperature is predicted within the next approximately 90 years. The range results from the different scenarios and considered seasons. Since Giorgi et al.[5] do not give clear guidance on how the air temperature distribution changes (e.g., if the standard deviation is changing as well), it is assumed that the distribution remains unchanged. Hence, each temperature value is increased by the same value of 1.8 to 2.9 K.

2.3 | Uncertainty modelling

To explain the required uncertainty modelling, a simplified example is introduced: We assume that the wind speed (x in this example) currently follows a normal distribution with the following distribution parameters $\theta = [\mu\ \sigma]^T$: mean value $\mu = 10$ ms^{-1} and standard deviation $\sigma = 2$ ms^{-1}. A change of the mean value of 3.5 to 4.5 ms^{-1} per decade is assumed to be predicted. This change is exaggerated for illustration purposes in Figure 3. The shape of distribution remains unchanged (i.e., σ is constant). For the avoidance of doubt, this exaggerated example is only used for illustration purposes is this section and not for the analyses in Section 4, where real data are used.

If no long-term changes of the environmental conditions are considered, the physical variability (or aleatory uncertainty) of these conditions is most frequently modelled using probability (PDF; $f(x|\theta)$) or cumulative density functions (CDF; $F(x|\theta)$). This procedure is described in Section 2.1. However, over time, climate change causes a variation of these distributions. Hence, distribution parameters θ change. At the same time, the model (epistemic) uncertainty increases. For our example, assuming a linear trend, after 10 years, the mean wind speed has increased by 3.5 to 4.5 ms^{-1}. After 20 years, the uncertainty interval is already 7 to 9 ms^{-1}.

To reproduce these two types of uncertainty (i.e., polymorphic uncertainty), interval random variables (i.e., imprecise probabilities) are applied. This means that the distribution parameters are no longer single values, but intervals $[\underline{\theta}, \bar{\theta}]$. For our example, the results after 10 years is

$$[\underline{\theta}_{10}, \bar{\theta}_{10}] = \begin{bmatrix} 13.5 & 14.5 \\ 2 & 2 \end{bmatrix}. \tag{3}$$

Accordingly, lower and upper PDFs can be defined for year n:

$$\underline{f}_n(x) = \min(f(x|\theta)) \text{ with } \underline{\theta}_n \le \theta \le \bar{\theta}_n \text{ and} \tag{4}$$

$$\bar{f}_n(x) = \max(f(x|\theta)) \text{ with } \underline{\theta}_n \le \theta \le \bar{\theta}_n. \tag{5}$$

For our example, the original PDF, the changed PDFs after one and two decades, and the corresponding uncertainty intervals are illustrated in Figure 3.

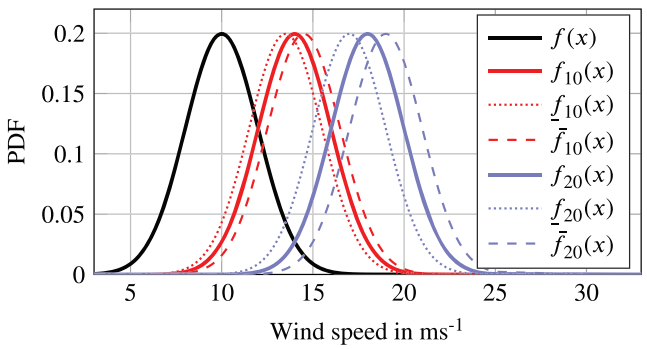

FIGURE 3 Illustration of interval definitions for PDFs due to increasing epistemic model uncertainty for three dates (today, in one decade, and in two decades). Effects are significantly exaggerated for illustration purposes [Colour figure can be viewed at wileyonlinelibrary.com]

3 | FATIGUE LIFETIME MODELLING

To efficiently analyse the impact of climate change on wind turbine fatigue lifetimes, three aspects have to be considered. First, a procedure to calculate fatigue lifetimes or at least a measure for lifetime fatigue damages is needed. Here, lifetime DELs[28] are utilised. Second, a suitable wind turbine model is required. Such a turbine is the NREL 5 MW reference wind turbine.[29] And last, to ensure an efficient computation, a meta-model, which correlates (polymorphic) uncertain environmental conditions to short-term DELs, is helpful. All three aspects are explained in the following in more detail.

3.1 | Damage equivalent loads

A short-term DEL represents a load signal with a constant frequency and amplitude (S_{eq}). It yields the same damage according to the Palmgren-Miner rule as an investigated (realistic) short-term load signal with various frequencies and amplitudes (S_i):

$$S_{eq} = \left(\sum \frac{n_i S_i^m}{N_{ref}} \right)^{-m}, \tag{6}$$

where $N_{ref} = 600$ to set the frequency of the DEL to 1 Hz for a 10-min period. S_i and n_i are different amplitudes and the corresponding number of cycles in the original load signal, when applying a rainflow counting. Material exponents are chosen as $m = 3$ for steel and $m = 10$ for composite materials in the rotor blades. Since the Palmgren-Miner rule is assumed to be valid, linear damage accumulation is presumed. For steel components, this assumption is widely valid. For rotor blades made of fibre-reinforced composites, its applicability is at least questionable.[30] Nonetheless, since fatigue modelling itself is not the focus of this work and DELs are still widely used in research and industry, we decided to stick with DELs as a measure of fatigue.

Short-term DELs give us a representative measure of fatigue for a short-time period (e.g., 10 min). However, to gain knowledge about fatigue lifetimes, DELs have to be calculated in the long term. For this purpose, a lifetime DEL[28] can be defined:

$$S_{eq,LT} = \left(\int S_{eq}(\mathbf{x})^m f(\mathbf{x}) d\mathbf{x} \right)^{-m}, \tag{7}$$

where $\mathbf{x}$ is the input vector of environmental conditions, that is, $\mathbf{x} = [v\ H_s\ T_p\ \rho]^T$, and $f(\mathbf{x})$ is the joint probability density function of $\mathbf{x}$. In this work, only operating conditions are considered. This means that, for example, no environmental conditions are considered, where the wind speed exceeds the cut-off wind speed of 25 ms^{-1} (see also Figure 6 (right)). Surely, this is a simplification of the actual situation. However, operating conditions contribute—at least for all steel components—most to fatigue. Moreover, other situations like rotor stops or fault cases depend significantly on the controller and turbine design and less on climate change. Therefore, they are less relevant for this study. Since the integral in Equation (7) cannot be solved analytically, normally, a finite number of random realisations of $\mathbf{x}$ is used to estimate $S_{eq,LT}$, that is, Monte Carlo integration.

If polymorphic uncertainty is considered and interval random variables $[\underline{\mathbf{x}}, \overline{\mathbf{x}}]$ are applied, short-term and lifetime DELs are also intervals: $[\underline{S}_{eq}, \overline{S}_{eq}]$ and $[\underline{S}_{eq,LT}, \overline{S}_{eq,LT}]$. In this context, an important fact is that $\underline{\mathbf{x}}$ does not necessarily yield $\underline{S}_{eq}$. For example, a low air density (i.e., $\underline{\mathbf{x}}$) can lead to low fatigue loads (i.e., $\underline{S}_{eq}$) due to a reduced rotor thrust (cf. Equation 2). However, it can also yield higher fatigue loads (i.e., $\overline{S}_{eq}$) due to decreased aerodynamic damping. Hence, the relationship is nonlinear. Therefore, for each realisation of $\mathbf{x}$, the minimum and the maximum value of S_{eq} has to be found:

$$\underline{S}_{eq}(\mathbf{x}) = \min(S_{eq}(\mathbf{x}) | \mathbf{x} \in [\underline{\mathbf{x}}, \overline{\mathbf{x}}]) \text{ and} \tag{8}$$

$$\overline{S}_{eq}(\mathbf{x}) = \max(S_{eq}(\mathbf{x}) | \mathbf{x} \in [\underline{\mathbf{x}}, \overline{\mathbf{x}}]). \tag{9}$$

Hence, a minimisation and a maximisation problem have to be solved for each realisation within the Monte Carlo integration. Here, they are solved using global optimisation by applying the global pattern search approach by Hofmeister et al.[31] A track number of $T = 2$ is chosen. A low track number results in a fairly local version of the global pattern search approach. This is reasonable, since there is only a low number of local minima in the 'truncated' objective spaces, that is, in $[\underline{\mathbf{x}}, \overline{\mathbf{x}}]$. A detailed and illustrative explanation of the optimisation problem embedded in the Monte Carlo integration for interval random variables is given by Hübler et al.[32]

3.2 | Wind turbine model

To determine the short-term DELs in Equation (6), load signals are required. In this work, load signals are simulated using the aero-hydro-servo-elastic simulation framework FASTv8[33] of the 'National Renewable Energy Laboratory' (NREL). Similarly to a reference site in Section 2.1, a reference turbine is required. Here, the NREL 5 MW reference wind turbine[29] with the OC3 monopile as substructure[34] is chosen (see Figure 4). A soil model that applies soil-structure interaction matrices[35] enhances the FASTv8 code. Soil conditions of the OC3 phase II model[34] are assumed. For all simulations, the simulation length is set to 10 min according to Hübler et al.[22] The 'run-in' time (i.e., the time that has to be removed from each time series to exclude initial transients) is set to 240 s.[22] The turbulent wind field is calculated using the Kaimal model. The JONSWAP spectrum is applied to compute irregular waves. Six relevant locations are selected to evaluate the load signals: shear force and overturning moment at mudline in (F_x and M_y) and perpendicular (F_y and M_x) to the wind direction and blade root bending moments ('in-plane' M_{IP} and 'out-of-plane' M_{OoP}). The locations are marked in Figure 4 together with the corresponding coordinate system.

3.3 | Meta-modelling

For the determination of long-term DELs, according to Equation (7), a multidimensional integration is required. As stated before, this integral is normally approximated by Monte Carlo integration, that is, a finite number of random realisations of $\mathbf{x}$. In case of interval random variables, an embedded optimisation has to be solved for each realisation (cf. Section 3.1). Ideally, the number of realisations corresponds to the number of 10-min periods in the entire lifetime of 25 years, that is, 1.3149×10^6. In this case, no load extrapolation techniques—adding additional uncertainties—are required. If applied, the embedded optimisation demands additional realisations, so that approximately 10^8 to 10^9 overall model evaluations are necessary. Since one model evaluation (i.e., one realisation of $S_{eq}(\mathbf{x})$ and therefore one time-domain simulation using the FASTv8 code) has a computing time of approximately 10 min, this procedure becomes inappropriate. Therefore, meta-models ($g(\mathbf{x})$), which approximate short-term DELs ($S_{eq}(\mathbf{x})$) by correlating the considered variable environmental conditions wind speed, wave height, wave period and air density with short-term DELs, are used in this work:

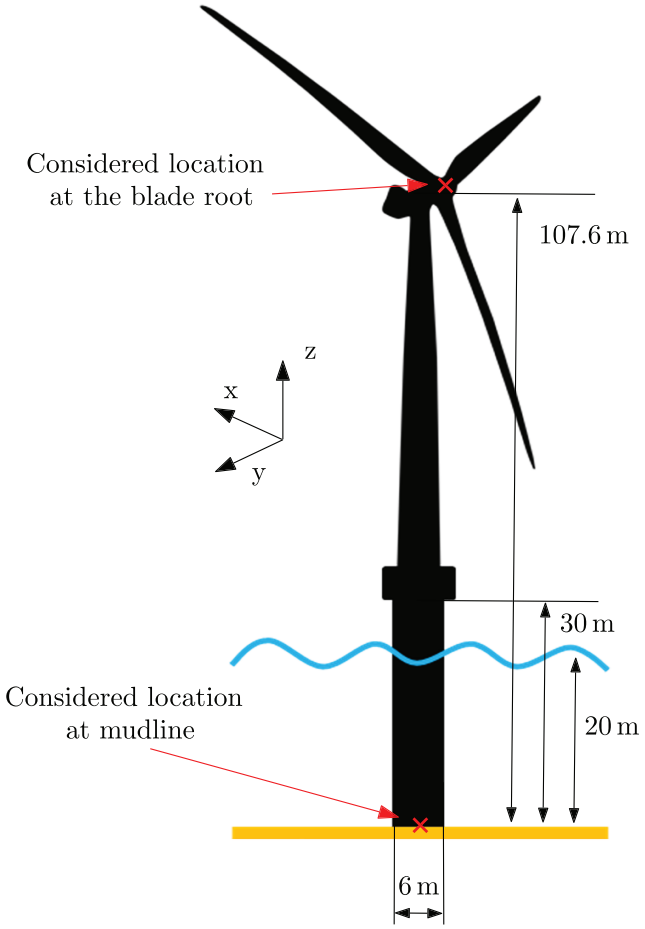

FIGURE 4 Visualisation of the OC3 monopile and the NREL 5 MW reference wind turbine (not to scale). Evaluated locations for load signals are marked. Inertial frame coordinate system: x downwind direction, y to the left when looking downwind and z vertically upwards [Colour figure can be viewed at wileyonlinelibrary.com]

$$\hat{S}_{eq}(\mathbf{x}) = g(v, H_s, T_p, \rho). \tag{10}$$

For this purpose, first, $n = n_{training} + n_{test} = 10000$ time-domain simulations using the FASTv8 code are conducted for random realisations of $\mathbf{x}$. This yields a data base of 10 000 short-term DELs and the corresponding environmental conditions. This simulation data base is published as an open-access data publication within the Research Data Repository of the Leibniz University Hannover (see Appendix A). Based on these data, in a second step, an own meta-model is created for each of the six considered loads. Meta-models for DELs gave promising results in the past.[28,36] Based on results of previous research and the results of Hübler and Rolfes,[32] a Kriging meta-model with a linear basis function and a squared exponential covariance function is set up. The Kriging model is fitted based on $n_{training} = 5000$ training data points. In a third step, the meta-models are validated based on another $n_{test} = 5000$ test data points. A visual validation for one exemplary load can be seen in Figure 5. Moreover, the normalised root-mean-square errors for the test data are calculated and summarised in Table 1:

$$\text{NRMSE} = \frac{1}{\text{E}(S_{eq}(\mathbf{x}))} \sqrt{\frac{\sum_{i=1}^{n_{test}} \left(\hat{S}_{eq}(\mathbf{x}_i) - S_{eq}(\mathbf{x}_i)\right)^2}{n_{test}}}, \tag{11}$$

where $\hat{S}_{eq}(\mathbf{x})$ is the short-term DEL predicted by the Kriging model.

Clearly, there are possible improvements regarding the meta-modelling especially for loads perpendicular to the wind direction. For these loads, wave effects become more relevant. Wave effects, especially resonance effects, are fairly nonlinear and therefore more challenging for meta-models. For possible improvements regarding meta-modelling, see for example Dimitrov et al[28] or Slot et al.[37] Moreover, in any case, meta-modelling adds an additional uncertainty to the lifetime DEL calculation. Although both are not focus of this work, the additional uncertainty will be discussed in Section 4.4.

4 | RESULTS

To determine the influence of climate change on the fatigue lifetime of offshore wind turbines, the methods presented in Sections 2 and 3 are applied to the described reference site and turbine. For the reference site, the present site conditions are determined. Subsequently, they are extrapolated for a planned wind turbine lifetime of 25 years. Finally, lifetime predictions based on the present site data and extrapolated conditions are conducted and compared to each other.

4.1 | Actual site data

For the FINO3 site and a measurement period of 8 years, postprocessed data are used to derive theoretical statistical distributions for wind speed, wave height, wave period and air density using the approach described in Section 2.1. Wind speed and air density are considered as independent

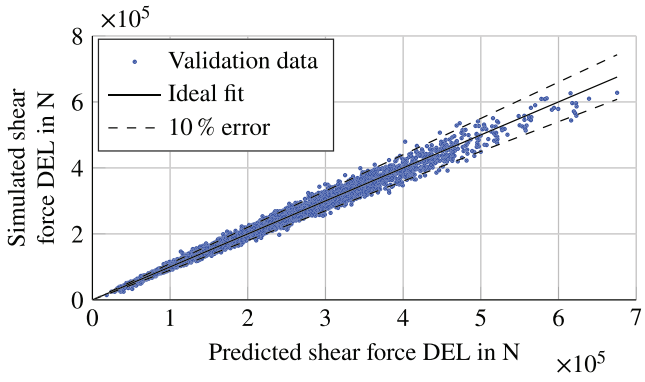

FIGURE 5 Visual validation of the Kriging model for F_x: Kriging prediction vs. aero-elastic simulation results [Colour figure can be viewed at wileyonlinelibrary.com]

TABLE 1 Normalised root-mean-square errors (NRMSE) for the test data for all six loads

Load	F_x	F_y	M_x	M_y	M_{IP}	M_{OoP}
NRMSE	0.059	0.120	0.274	0.075	0.003	0.073

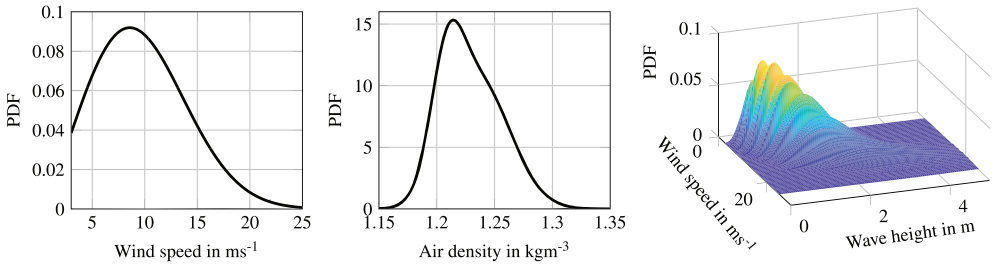

FIGURE 6 Probability density functions (PDFs) for wind speed (left), air density (middle) and significant wave height (right) for the FINO3 site. For the wave height, the noncontinuous joint PDF (wind speed-wave height PDF) is given. Corresponding distribution types and parameters are given in Appendix B [Colour figure can be viewed at wileyonlinelibrary.com]

variables. For the wave height, several distributions are defined for different wind speed bins. For the wave period, distributions change depending on the wave height. The distributions of wind speed and air density are shown in Figure 6 (left and middle). In addition, for some wind speed bins, the corresponding wave height distributions are displayed in Figure 6 (right). All distribution types and parameters are summarised in Appendix B.

The theoretical distributions given in Figure 6 represent the empirical distributions of the given 8-year period relatively well. Still, there is some statistical uncertainty due to limited data especially for dependent variables.[32] Since climate change is expected for the upcoming years, the validity of these distributions for the next 25 years, that is, the planned lifetime of a wind turbine constructed today, is not approved.

4.2 | Predicted site data

In Section 2.2, three different models for climate change are presented. Two models focus on increasing median and extreme (99th percentile) wind speeds[13,14] and one on increasing air temperatures.[5] In the following, the models based on Zeng et al,[14] Grabemann and Weisse[13] and Giorgi et al[5] are called *MedWind*, *ExtWind* and *Temp*, respectively. All three models are applied to predict the change of the distributions determined in the last section. Only for the *MedWind* model, a change per decade is explicitly stated. For the other two models, predictions for the period 2071-2100 are given. To calculate changes per decade and finally yearly changes, we assume a linear increase reaching the given predictions in 90 years. Surely, this assumption is an unvalidated simplification. The real change is expected to be nonlinear. Nonetheless, first, this assumption is probably conservative, since an acceleration of the changes is predicted. Hence, changes in the next 25 years will be slightly lower. And second, if necessary for further investigations, models for climate change can easily be interchanged making analyses more precise. The resulting changes per decade are summarised in Table 2. In addition, upper and lower limits of changes per decade due to the uncertainty in the predictions are given.

Based on these changes, theoretical distributions are determined for each year within the 25-year lifetime. As explained in Section 2.2.3, for the air temperature change, it is assumed that the whole distribution is shifted. For this purpose, each temperature value in the original data is increased by the corresponding Δ_T value. Subsequently, for each year, a distribution is fitted to the data. The resulting air density distribution after 25 years is shown in Figure 7 (middle). Lower and upper limits are given as well. For the wind speed, changes are given for the median and the 99th percentile. It is assumed that the type of distribution (here Weibull distribution) remains unchanged. Then, using numerical optimisation, new distribution parameters, which yield the required values for the median and the 99th percentile, are calculated. This procedure leads to a change of the shape of the distribution, since extreme wind speeds become more probable (i.e., the standard deviation of the distribution is increased).

TABLE 2 Predicted changes per decade for median ($\Delta_{v,50}$) and extreme ($\Delta_{v,99}$) wind speed and air temperature (Δ_T) at the FINO3 site based on the three models *MedWind*, *ExtWind* and *Temp* based on Zeng et al,[14] Grabemann and Weisse,[13] and Giorgi et al,[5] respectively

	MedWind	*ExtWind*	*Temp*
$\Delta_{v,50}$ in ms^{-1}	0.24	0.008	0
$\Delta^{\pm}_{v,50}$ in ms^{-1}	0.12 - 0.36	–0.003 - 0.019	0
$\Delta_{v,99}$ in ms^{-1}	0.24	0.082	0
$\Delta^{\pm}_{v,99}$ in ms^{-1}	0.12 - 0.36	0.050 - 0.11	0
Δ_T in K	0	0	0.27
$\Delta^{\pm}_T$ in K	0	0	0.20 - 0.32

Note: Ranges ($\Delta^{\pm}$) due to the uncertainty of the predictions are given as well.

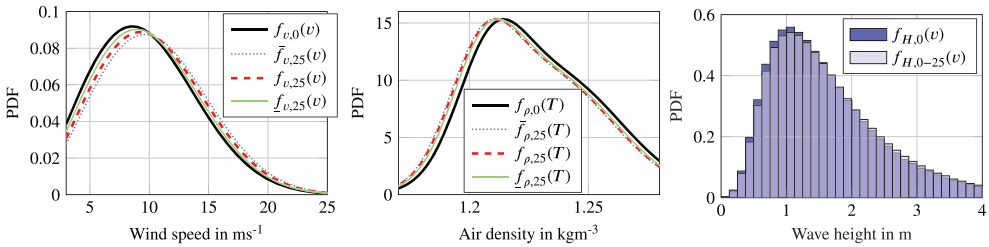

FIGURE 7 Probability density functions (PDFs) for wind speed (left) and air density (middle) for the FINO3 site today (f_0) and in 25 years (f_{25}). Twenty five-year prediction is based on the *MedWind* and *Temp* model, respectively. Lower and upper limits due to the uncertainty in the predictions are given. For the wave height (right), normalised histograms showing the occurrence probability over 25 years are given assuming no wind speed change ($f_{H,0}(v)$) or a linear increase according to the *MedWind* model ($f_{H,0-25}(v)$) [Colour figure can be viewed at wileyonlinelibrary.com]

TABLE 3 Percentage differences in lifetime DELs of the four climate change models compared to the reference model (*Ref*) for two loads: overturning moment at mudline in wind direction (M_y) and the 'out-of-plane' blade root bending moment (M_{OoP})

	ΔM_y in %	ΔM_{OoP} in %
MedWind	1.01	1.58
	−0.08 - 2.08	0.71 - 2.37
ExtWind	0.20	0.53
	0.03 - 0.32	0.27 - 0.67
MedWindTemp	1.04	1.48
	−0.07 - 2.11	0.63 - 2.24
ExtWindTemp	0.23	0.47
	0.04 - 0.35	0.20 - 0.61

Note: Ranges due to the uncertainty of the climate change models are given.

This fact is illustrated in Figure 7 (left). Wave height and wave period distributions are assumed to be constant. It should be noted that this does not mean that wave heights do not increase over time. Since wind speeds increase and wave heights depend on the wind speed, higher wave heights are predicted even for constant wave height distributions. An illustration of increasing wave heights is given in Figure 7 (right). The assumption of increasing wind speeds ($f_{H,0-25}(v)$) leads to slightly higher wave heights compared to a constant wind speed distribution ($f_{H,0}(v)$).

4.3 | Lifetime prediction

As a measure of the fatigue lifetime of the considered reference turbine, lifetime DELs based on Equation (7) are used. This equation is approximated using Monte Carlo integration. Meta-models are applied for the calculation of the short-term DELs (cf. Section 3.3). The required random realisations of $\mathbf{x}$, that is, of the environmental conditions, are based on the theoretical distributions determined in the previous section. Since the distributions change over time, for each year, individual distributions are used. The 1.3149×10^6 samples corresponding to 25 years are split up into separate years. For each year, 52 596 samples are drawn from the corresponding distributions. Subsequently, Equation (7) is evaluated by means of the meta-models (and a global optimisation in case of interval random variables).

Five different cases are considered: No climate change (*Ref*), increase of the wind speed according to Zeng et al[14] (*MedWind*) and Grabemann and Weisse[13] (*ExtWind*), and increase of wind speed and air temperature (*MedWindTemp* and *ExtWindTemp*). For each of these five cases, predicted lifetime DELs of all six loads are calculated together with lower and upper limits representing the inherent uncertainty. For the overturning moment at mudline in wind direction (M_y) and the 'out-of-plane' blade root bending moment (M_{OoP}), percentage differences in lifetime DELs of the four climate change models compared to the reference model (i.e., the model, which assumes no climate change (*Ref*)) are given in Table 3. For all other loads, results are summarised in Appendix B.

Analysing the results in Table 3 and the additional outcomes summarised in Table C1 in Appendix B, several trends become clear. First and most important, independent of the model, the increase in lifetime DELs is below 5% and therefore fairly small. Second, the uncertainty in the prediction compared to the change itself is quite high. For example, for the *MedWind* model, the overturning moment changes between zero and two percent, while an increase of 1% is predicted. This is an uncertainty of ±100%. And third, the increasing air temperature has nearly no influence on fatigue loads. It can lead to slightly higher and lower lifetime DELs, since decreasing air densities reduce aerodynamic loads and damping at the same time. Which effect is dominating, depends on the considered load but also on the actual wind speed, etc.

4.4 | Other uncertainties

In the previous section, it was demonstrated that the influence of climate change on lifetime DELs and therefore on fatigue lifetimes is limited. Before we draw conclusions regarding the relevance of including climate change models into lifetime calculations, an analysis of other uncertainties in this process is valuable. Only if effects of climate change are comparably relevant compared to other uncertainties, the inclusion of climate change models provides an additional value. In this section, three different types of uncertainties are considered exemplarily: the uncertainty of the meta-model, the uncertainty of the lifetime calculation/extrapolation and the uncertainty of the initial (unextrapolated) distributions. Surely, there are several other uncertainties, which might also be important. However, the selected three uncertainties already clarify the present challenge.

Regarding the uncertainty of the meta-model, Figure 5 shows that uncertainties in short-term DELs of up to 10% are not uncommon. Of course, more sophisticated meta-models can decrease this uncertainty. However, up to now, errors of lifetime DELs remain around 5%.[28] This might change in future, while meta-models become even more accurate.

To eliminate the uncertainty of meta-modelling, lifetime calculations can also be based on aero-elastic simulations instead. In this case, it is not practical to conduct 1.3149×10^6 simulations to model the entire lifetime. Much fewer simulations are conducted (e.g., 10 000). Then, results are extrapolated. In Hübler et al,[38] it is shown that such extrapolations lead to errors due to finite sampling of at least 5–10%. In many cases, the extrapolation uncertainty is even much higher. Hence, this is no alternative to reduce the overall uncertainty. At this point, it should be mentioned that even without any extrapolation, there is some uncertainty due to finite sampling. This uncertainty is a result of the random selection of the 1.3149×10^6 samples in 25 years. However, this uncertainty is only around 0.1% and therefore negligible.[32]

Effects of the uncertainty of the initial (unextrapolated) distributions on lifetime DELs have recently been investigated.[32] It was shown that this uncertainty highly depends on the uncertainty model itself. Nonetheless, it was concluded that—especially if an insufficient amount of data is available, which is frequently the case for high wind speed bins—distributions of dependent variables feature a high amount of uncertainty. This uncertainty propagates through the entire lifetime calculation. Resulting uncertainties of the lifetime DELs are around 10%. Although it might be possible to reduce this type of uncertainty using more advanced methods determining the statistical distributions of the environmental conditions, without further research, it is clearly relevant in this context.

To summarise: Uncertainties within the fatigue lifetime calculation are in general higher than the predicted variation due to climate change. This poses a challenge for the incorporation of climate change models into lifetime calculations. Only if meta-models or extrapolation techniques are improved and very comprehensive site data are available or the modelling of site-specific environmental conditions is enhanced, climate change models can actually improve lifetime calculations.

4.5 | Concluding results

In this section, we draw conclusions regarding the relevance of including climate change models into current lifetime calculations.

First, climate change has an identifiable but fairly small influence on the fatigue lifetime of offshore wind turbines in the North Sea. The inherent uncertainty of this influence is quite large compared to the effect itself. The influence is mainly driven by increasing wind speeds and not by rising air temperatures. Air temperature variations have a negligible effect.

Second, if there is an influence, is it relevant as well? Regarding this question, it has to be concluded that climate change does not have to be considered in current lifetime calculations in the first place. Present meta-models, approaches to determine distributions for environmental conditions, etc. lead to uncertainties that exceed all effects of climate change modelling.

5 | BENEFITS AND LIMITATIONS

Recently, it has been forecasted that wind speeds will increase over the next few decades again. The influence of these increasing wind speeds and other effects of climate change on fatigue loads of offshore wind turbines has been analysed in this work for the first time ever. Since predictions regarding climate change are fairly uncertain, the present analysis incorporated an uncertainty quantification. It was shown that—using current models and approaches—the use of climate change models within lifetime calculations of offshore wind turbines has no pronounced additional value. Hence, such effects should either be neglected within turbine design or further developments are required to reduce other uncertainties.

The present study is based on several assumptions and simplifications. For example, all investigations might be site- and turbine-dependent. Here, only a single site in the North Sea and a reference turbine are analysed. For sites outside the North Sea, for which much higher changes are predicted, the results might be different. Nonetheless, the feature that significant changes in wind speeds (e.g., 0.6 ms^{-1} in 25 years) only lead to marginal changes in lifetime DELs (+1.01% for ΔM_y) is probably relatively generally valid. Moreover, DELs are only calculated based on operating conditions. Real storms above cut-off wind speed are not considered. However, they are normally less relevant for fatigue. In addition, it should

be mentioned that both the utilised meta-model and the concept of using DELs for rotor blades lead to model uncertainties that are not explicitly considered within the lifetime calculation in this study. For the general conclusions of this study, these uncertainties should not be relevant or even reinforce them, since effects of climate change might become even less relevant. Moreover, this study focussed on fatigue loads and not on extreme loads. This is reasonable, since fatigue is normally design-driving for most components (e.g., all parts made of steel). Nonetheless, for rotor blades and in regions with hurricanes etc., an additional study for extreme loads would be valuable, especially since extreme weather conditions are predicted to become more probable. Finally, it should be noted that effects of climate change on fatigue lifetimes might become more relevant for the next generation of large turbines (≥8 MW) with, for example, very flexible blades and more nonlinear coupling effects like blade bending and twisting etc.

6 | CONCLUSIONS

While wind energy has the potential to reduce green house gas emissions, and therefore has an influence on climate change, the inverted effect of climate change on wind turbines is less analysed so far. Some previous studies focussed on potential changes in the wind energy production potential, but influences on wind turbine loads are nearly unexplored. In this work, effects of increasing wind speeds and air temperatures over the next 25 years were investigated for wind turbines in the North Sea. It was shown that fatigue loads will increase slightly (below 5%). Nonetheless, as other uncertainties in the lifetime calculation are significantly larger, an inclusion of effects of climate change into lifetime calculations is currently not necessary. This might change if lifetime calculations become more accurate—resulting in less conservative design—or if climate change becomes more severe.

ACKNOWLEDGEMENTS

We gratefully acknowledge the financial support of the Deutsche Forschungsgemeinschaft (DFG, German Research Foundation) for the *ENERGIZE* project (436547100). Open access funding enabled and organized by Projekt DEAL.

PEER REVIEW

The peer review history for this article is available at https://publons.com/publon/10.1002/we.2572.

DATA AVAILABILITY STATEMENT

The raw data for the exemplary site are taken from the FINO3 platform—currently operated by the 'The FuE-Zentrum FH Kiel GmbH' on behalf of Federal Ministry of Economics Affairs and Energy (BMWi). The data are freely available for research purposes (https://www.fino3.de/en/).

The simulation data, which are used to construct the meta-models, are published as an open-access data publication within the Research Data Repository of the Leibniz University Hannover: https://doi.org/10.25835/0078042

ORCID

Clemens Hübler https://orcid.org/0000-0001-7191-4369

REFERENCES

1. International Energy Agency. Offshore Wind Outlook. International Energy Agency (IEA). Technical report, France; 2019. https://www.iea.org/reports/offshore-wind-outlook-2019
2. Bindoff NL, Stott PA, Achuta Rao KM, et al. Detection and attribution of climate change: From global to regional. *Climate Change 2013: The Physical Science Basis. Contribution of Working Group I to the Fifth Assessment Report of the Intergovernmental Panel on Climate Change*. Cambridge, United Kingdom and New York, NY, USA: Cambridge University Press; 2013:867-952.
3. McVicar TR, Roderick ML, Donohue RJ, et al. Global review and synthesis of trends in observed terrestrial near-surface wind speeds: implications for evaporation. *J Hydrol*. 2012;416:182-205.
4. Sévellec F, Drijfhout SS. A novel probabilistic forecast system predicting anomalously warm 2018-2022 reinforcing the long-term global warming trend. *Nature Commun*. 2018;9(1):1-12.
5. Giorgi F, Bi X, Pal J. Mean, interannual variability and trends in a regional climate change experiment over Europe II: climate change scenarios (2071–2100). *Climate Dyn*. 2004;23(7-8):839-858.
6. Pryor SC, Barthelmie RJ. Climate change impacts on wind energy: a review. *Renew Sustain Energy Rev*. 2010;14(1):430-437.
7. Roderick ML, Rotstayn LD, Farquhar GD, Hobbins MT. On the attribution of changing pan evaporation. *Geophys Res Lett*. 2007;34(17):L17403.
8. Vautard R, Cattiaux J, Yiou P, Thépaut JN, Ciais P. Northern Hemisphere atmospheric stilling partly attributed to an increase in surface roughness. *Nature Geosci*. 2010;3(11):756-761.
9. Tian Q, Huang G, Hu K, Niyogi D. Observed and global climate model based changes in wind power potential over the Northern Hemisphere during 1979–2016. *Energy*. 2019;167:1224-1235.
10. Tobin I, Jerez S, Vautard R, et al. Climate change impacts on the power generation potential of a European mid-century wind farms scenario. *Environ Res Lett*. 2016;11(3):34013.

11. Quante M, Colijn F. *North Sea Region Climate Change Assessment*. Switzerland: Springer Nature; 2016.
12. Pryor SC, Schoof JT, Barthelmie RJ. Winds of change?: projections of near-surface winds under climate change scenarios. *Geophys Res Lett*. 2006;33 (11):L11702.
13. Grabemann I, Weisse R. Climate change impact on extreme wave conditions in the North Sea: an ensemble study. *Ocean Dyn*. 2008;58(3-4):199-212.
14. Zeng Z, Ziegler A, Searchinger T, et al. A reversal in global terrestrial stilling and its implications for wind energy production. *Nat Clim Change*. 2019;9 (12):979-985.
15. Tobin I, Vautard R, Balog I, et al. Assessing climate change impacts on European wind energy from ENSEMBLES high-resolution climate projections. *Clim Change*. 2015;128(1-2):99-112.
16. International Electrotechnical Commission. *Wind Energy Generation Systems - Part 1: Design Requirements*. Geneva, Switzerland: International Electrotechnical Commission (IEC); 2019.
17. Clausen NE, Gryning SE, Larsén XG, et al. Impact from climate change on extreme winds and icing conditions in the Baltic Region. In: Proceedings of Copenhagen Offshore Wind; 2005; Copenhagen, Denmark.
18. Clausen NE, Lundsager P, Barthelmie R, Holttinen H, Laakso T, Pryor SC. Wind Power. *Impacts of Climate Change on Renewable Energy Sources*. Copenhagen, Denmark: Norden; 2007:105-128.
19. Bisoi S, Haldar S. Effect of climate change on dynamic behavior of monopile supported offshore wind turbine structure. *Japanese Geotechnical Society Special Publication*. 2016;2(33):1189-1193.
20. Bisoi S, Haldar S. Impact of climate change on dynamic behavior of offshore wind turbine. *Marine Geores Geotechnol*. 2017;35(7):905-920.
21. https://www.fino3.de/en/ (last access: May 2020).
22. Hübler C, Gebhardt CG, Rolfes R. Development of a comprehensive database of scattering environment conditions and simulation constraints for offshore wind turbines. *Wind Energy Sci*. 2017;2:491-505.
23. Hübler C, Gebhardt CG, Rolfes R. Hierarchical four-step global sensitivity analysis of offshore wind turbines based on aeroelastic time domain simulations. *Renew Energy*. 2017;111:878-891.
24. Stewart GM, Robertson R, Jonkman J, Lackner MA. The creation of a comprehensive metocean data set for offshore wind turbine simulations. *Wind Energy*. 2016;19(6):1151-1159.
25. Fischer T, De Vries W, Schmidt B. Upwind Design Basis. Upwind Deliverable (WP4: Offshore Foundations and Support Structures). Endowed Chair of Wind Energy (SWE) at the Institute of Aircraft Design Universit at Stuttgart. Technical report, Germany; 2010. https://repository.tudelft.nl/islandora/object/uuid%3Aa176334d-6391-4821-8c5f-9c91b6b32a27
26. Li L, Gao Z, Moan T. Joint distribution of environmental condition at five european offshore sites for design of combined wind and wave energy devices. *J Offshore Mech Arct Eng*. 2015;137(3):31901.
27. Johannessen K, Meling TS, Hayer S. Joint distribution forwind and waves in the northern north sea. *Int J Offshore Polar Eng*. 2002;12(1):1-8.
28. Dimitrov NK, Kelly MC, Vignaroli A, Berg J. From wind to loads: wind turbine site-specific load estimation with surrogate models trained on high-fidelity load databases. *Wind Energy Sci*. 2018;3:767-790.
29. Jonkman J, Butterfield S, Musial W, Scott G. Definition of a 5-MW reference wind turbine for offshore system development. NREL/TP-500-38060, Golden, Colorado USA, National Renewable Energy Laboratory; 2009.
30. Krüger H, Rolfes R. A physically based fatigue damage model for fibre-reinforced plastics under plane loading. *Int J Fatig*. 2015;70:241-251.
31. Hofmeister B, Bruns M, Rolfes R. Finite element model updating using deterministic optimisation: a global pattern search approach. *Eng Struct*. 2019; 195:373-381.
32. Hübler C, Rolfes R. Polymorphic uncertainty in met-ocean conditions and the influence on fatigue loads . 2020.
33. Jonkman J. The new modularization framework for the FAST wind turbine CAE tool. In: 51St AIAA Aerospace Sciences Meeting, including the New Horizons Forum and Aerospace Exposition; 2013; Dallas, Texas, US:202.
34. Jonkman JM, Musial W. Offshore Code Comparison Collaboration (OC3) for IEA Task 23 Offshore Wind Technology. NREL/TP-5000-48191, Golden, Colorado, USA, National Renewable Energy Laboratory; 2010.
35. Häfele J, Hübler C, Gebhardt CG, Rolfes R. An improved two-step soil-structure interaction modeling method for dynamical analyses of offshore wind turbines. *Appl Ocean Res*. 2016;55:141-150.
36. Müller K, Cheng PW. A surrogate modeling approach for fatigue damage assessment of floating wind turbines. In: ASME 2018 37th International Conference on Ocean, Offshore and Arctic Engineering; 2018; Madrid, Spain: V010T09A065.
37. Slot RM, Sørensen JD, Sudret B, Svenningsen L, Thøgersen ML. Surrogate model uncertainty in wind turbine reliability assessment. *Renew Energy*. 2020;151:1150-1162.
38. Hübler C, Gebhardt CG, Rolfes R. Methodologies for fatigue assessment of offshore wind turbines considering scattering environmental conditions and the uncertainty due to finite sampling. *Wind Energy*. 2018;21(11):1092-1105.

How to cite this article: Hübler C, Rolfes R. Analysis of the influence of climate change on the fatigue lifetime of offshore wind turbines using imprecise probabilities. *Wind Energy*. 2021;24:275–289. https://doi.org/10.1002/we.2572

APPENDIX A: DISTRIBUTION PARAMETERS FOR ACTUAL SITE DATA

In this appendix, the distribution parameters for all distributions determined in Section 4.1 are given.

Wind speed:

Dependencies: none

Distributions: Weibull (truncated at 3 and 25 ms^{-1})

$$f(x|k,\lambda) = \begin{cases} \frac{k}{\lambda}\left(\frac{x}{\lambda}\right)^{k-1} e^{-\left(\frac{x}{\lambda}\right)^k} & \text{for } x \geq 0 \\ 0 & \text{for } x < 0. \end{cases} \tag{B1}$$

Distribution parameters: given in Table B1

Air density:

Dependencies: none

Distributions: bimodal log-normal

$$\begin{aligned} f(x|p,\mu_1,\mu_2,\sigma_1,\sigma_2) &= p\frac{1}{x\sigma_1\sqrt{2\pi}} e^{-\frac{(\ln(x)-\mu_1)^2}{2\sigma_1^2}} \\ &\quad + (1-p)\frac{1}{x\sigma_2\sqrt{2\pi}} e^{-\frac{(\ln(x)-\mu_2)^2}{2\sigma_2^2}}. \end{aligned} \tag{B2}$$

Distribution parameters: given in Table B2

Significant wave height:

Dependencies: wind speed

Distributions: gamma and extreme value (maximum)

$$f(x|k,\theta) = \frac{1}{\Gamma(k)\theta^k} x^{k-1} e^{-\frac{x}{\theta}} \text{ and} \tag{B3}$$

$$f(x|\mu,\beta) = \frac{1}{\beta} e^{-\frac{x+\mu}{\beta}} e^{-e^{-\frac{x+\mu}{\beta}}}. \tag{B4}$$

Distribution parameters: given in Table B3

Wave peak period:

Dependencies: wave height

Distributions: bimodal extreme value (maximum)

$$\begin{aligned} f(x|p,\mu_1,\mu_2,\beta_1,\beta_2) &= p\frac{1}{\beta_1} e^{-\frac{x+\mu_1}{\beta_1}} e^{-e^{-\frac{x+\mu_1}{\beta_1}}} \\ &\quad (1-p)\frac{1}{\beta_2} e^{-\frac{x+\mu_2}{\beta_2}} e^{-e^{-\frac{x+\mu_2}{\beta_2}}}. \end{aligned} \tag{B5}$$

Distribution parameters: given in Table B4

TABLE B1 Statistical parameters of the wind speed distribution

Distribution	k	λ
Weibull	2.3249	10.9221

TABLE B2 Statistical parameters of the air density distribution

Distribution	p	μ_1	μ_2	σ_1	σ_2
Bimodal log-normal	0.3192	0.1897	0.2133	0.0117	0.0216

TABLE B3 Statistical distributions and their parameters for the significant wave height depending on the wind speed

Wind speed in ms^{-1}	Distribution	k	θ	μ	β
2 – 4	Extreme value	-	-	–0.6574	0.3134
4 – 6	Extreme value	-	-	–0.7384	0.3344
6 – 8	Extreme value	-	-	–0.9072	0.3803
8 – 10	Gamma	7.0524	0.1948	-	-
10 – 12	Gamma	7.8838	0.2148	-	-
12 – 14	Gamma	8.5426	0.2377	-	-
14 – 16	Gamma	8.3262	0.2975	-	-
16 – 18	Gamma	12.1001	0.2457	-	-
18 – 20	Gamma	13.2347	0.2675	-	-
20 – 22	Gamma	14.2778	0.2895	-	-
22 – 24	Gamma	25.4950	0.1990	-	-
24 – 26	Gamma	31.4446	0.1708	-	-

TABLE B4 Statistical parameters of the wave peak period distribution depending on the wave height

Wave height in m	Distribution	p	μ_1	μ_2	σ_1	σ_2
0.0 – 0.5	Bimodal extreme value	0.6053	–3.9626	–9.6905	1.0930	1.8538
0.5 – 1.0	Bimodal extreme value	0.6638	–4.6603	–10.0790	1.0185	2.0736
1.0 – 1.5	Bimodal extreme value	0.8207	–5.4593	–10.2861	0.9346	1.5219
1.5 – 2.0	Bimodal extreme value	0.8333	–6.1431	–8.2518	0.8892	1.8590
2.0 – 2.5	Bimodal extreme value	0.1697	–5.9281	–7.3713	0.3110	0.8724
2.5 – 3.0	Bimodal extreme value	0.1687	–6.4572	–7.9640	0.3089	0.7274
3.0 – 3.5	Bimodal extreme value	0.1257	–6.9451	–8.4853	0.3478	0.7700
3.5 – 4.0	Bimodal extreme value	0.3759	–8.5794	–8.9802	1.1084	0.6060
4.0 – 4.5	Bimodal extreme value	0.4763	–9.5501	–9.6170	1.0189	0.5989
4.5 – 5.0	Bimodal extreme value	0.7492	–10.1678	–10.0311	0.9665	0.2020
5.0 – 5.5	Bimodal extreme value	0.0405	–9.1045	–10.6642	0.1413	0.7275
5.5 – 6.0	Bimodal extreme value	0.8880	–10.9433	–13.4173	0.7736	0.1094
6.0 – 6.5	Bimodal extreme value	0.1526	–10.6463	–11.8768	0.0049	0.8003

APPENDIX B: ADDITIONAL LIFETIME PREDICTION RESULTS

In this appendix, lifetime results in addition to Table 3 are given for the overturning moment at mudline perpendicular to the wind direction (M_x), the 'in-plane' blade root bending moment (M_{IP}) and the shear force in (F_x) and perpendicular (F_y) to the wind direction. The additional results are summarised in Table C1.

TABLE C1 Percentage differences in lifetime DELs of the four climate change models compared to the reference model (i.e., the model, which assumes no climate change (*Ref*)) for four loads: the overturning moment at mudline perpendicular to the wind direction (M_x), the 'in-plane' blade root bending moment (M_{IP}) and the shear force in (F_x) and perpendicular (F_y) to the wind direction

	ΔM_x in %	ΔM_{IP} in %	ΔF_x in %	ΔF_y in %
MedWind	2.29	0.21	2.03	3.24
	0.58–3.96	0.11–0.32	0.96–2.99	1.28–5.14
ExtWind	0.40	0.02	0.34	0.70
	0.10–0.63	0.01–0.04	0.13–0.43	0.31–1.00
MedWindTemp	2.31	0.21	2.03	3.19
	0.60–4.00	0.10–0.32	0.97–2.99	1.24–5.08
ExtWindTemp	0.42	0.02	0.34	0.67
	0.12–0.66	0.00–0.04	0.13–0.43	0.27–0.96